Functional and Topological Studies with Trp-Containing Analogs of the Peptide StII(1-30) Derived From the N-Terminus of the Pore Forming Toxin Sticholysin II: Contribution to Under...

ARTICLE *in* BIOPOLYMERS · JULY 2013

Impact Factor: 2.39 · DOI: 10.1002/bip.22211 · Source: PubMed

9 AUTHORS, INCLUDING:

Eduardo Cilli
São Paulo State University
87 PUBLICATIONS **809** CITATIONS
SEE PROFILE

Maria Eliana Lanio
University of Havana
79 PUBLICATIONS **1,164** CITATIONS
SEE PROFILE

Shirley Schreier
University of São Paulo
145 PUBLICATIONS **3,696** CITATIONS
SEE PROFILE

Carlos Alvarez
University of Havana
73 PUBLICATIONS **994** CITATIONS
SEE PROFILE

Functional and Topological Studies with Trp-Containing Analogs of the Peptide StII$_{1-30}$ Derived From the N-Terminus of the Pore Forming Toxin Sticholysin II: Contribution to Understand its Orientation in Membrane

Uris Ros,[1] Ana Lucia C. F. Souto,[2] Felipe J. de Oliveira,[2] Edson Jr. Crusca,[3] Fabiola Pazos,[1] Eduardo M. Cilli,[3] Maria E. Lanio,[1] Shirley Schreier,[2] Carlos Alvarez[1]

[1]*Center for Protein Studies, Biology Faculty, University of Havana (UH), Havana, Cuba*

[2]*Department of Biochemistry, Institute of Chemistry, University of São Paulo (USP), São Paulo, Brazil*

[3]*Department of Biochemistry and Chemical Technology, Institute of Chemistry, São Paulo State University (UNESP), Araraquara, São Paulo, Brazil*

Received 5 September 2012; revised 14 December 2012; accepted 14 January 2013
Published online 19 July 2013 in Wiley Online Library (wileyonlinelibrary.com). DOI 10.1002/bip.22211

ABSTRACT:

Sticholysin II (St II) is the most potent cytolysin produced by the sea anemone Stichodactyla helianthus, *exerting hemolytic activity via pore formation in membranes. The toxin's N-terminus contains an amphipathic α-helix that is very likely involved in pore formation. We have previously demonstrated that the synthetic peptide StII$_{1-30}$ encompassing the 1–30 segment of St II forms pores of similar radius to that of the protein (around 1 nm), being a good model of toxin functionality. Here we have studied the functional and conformational properties of fluorescent analogs of StII$_{1-30}$ in lipid membranes. The analogs were obtained by replacing Leu residues at positions 2, 12, 17, and 24 with the intrinsically fluorescent amino acid Trp (StII$_{1-30L2W}$, StII$_{1-30L12W}$, StII$_{1-30L17W}$, or StII$_{1-30L24W}$, respectively). The exchange by Trp did not significantly modify the activity and conformation of the parent peptide. The blue-shift and intensity enhancement of fluorescence in the presence of membrane indicated that Trp at position 2 is more deeply buried in the hydrophobic region of the bilayer. These experiments, as well as assays with water-soluble or spin-labeled lipid-soluble fluorescence quenchers suggest an orientation of StII$_{1-30}$ with its N-terminus oriented towards the hydrophobic core of the bilayer while the rest of the peptide is more exposed to the aqueous environment, as hypothesized for sticholysins.* © *2013 Wiley Periodicals, Inc. Biopolymers (Pept Sci) 100: 337-346, 2013.*

Keywords: sticholysin; pore-forming toxin; Trp-containing peptides; transbilayer orientation; fluorescence

This article was originally published online as an accepted preprint. The "Published Online" date corresponds to the preprint version. You can request a copy of the preprint by emailing the Biopolymers editorial office at biopolymers@wiley.com

INTRODUCTION

Sticholysins (StI and StII) are two pore-forming toxins purified from *Stichodactyla helianthus*,[1] which belong to the group of actinoporins,[2] a term used to describe cytolytic polypeptides produced by sea anemones. Actinoporins are characterized by being

Additional Supporting Information may be found in the online version of this article.

Correspondence to: Carlos Alvarez; e-mail: calvarez@fbio.uh.cu

Contract grant sponsor: CAPES-MES and CNPq-MES (Brazil-Cuba) Collaboration Projects
Contract grant sponsor: Iberoamerican CYTED BIOTOX Network
Contract grant number: 212RT0467
Contract grant sponsor: IFS, Sweden
Contract grant number: 4616

cysteineless proteins, with molecular weight around 20 kDa, and high affinity for sphingomyelin (SM).[3] The conformational changes experienced by actinoporins triggered by binding to membranes, the membrane-induced damage, and the nature of the pore formed by these toxins are not fully understood. The 3D structure of StII[4] as well as those of three other highly homologous actinoporins: StI,[5] equinatoxin II (EqtII),[6,7] and fragaceatoxin C (FraC)[8] have been solved by X-ray crystallography or NMR. Those studies revealed that actinoporins are characterized by a common fold containing a hydrophobic β-sandwich core, flanked on opposite sides by two α-helices. Crystallographic data have shown that in St II these α-helices comprise residues 14–23 and 128–135. Furthermore, residues 14–23 of St II form an amphipathic α-helix. The N-terminal sequence encompassing residues 1–30, which includes one of these helices, seems to detach from the toxin's main body, being the best candidate for pore formation.[4] Very likely the N-termini of actinoporins play an important role in pore formation by inducing redistribution of the lipid molecules. This membrane reorganization seems to render a toroidal pore whose lumen would be lined with the hydrophilic face of the amphipathic α-helix, and the polar head groups of phospholipids.[9–11] However, recently Mechaly et al. have postulated a new model for the pore formed by FraC, in which the channel structure is assembled by nine FraC N-termini with no lipid involvement in the pore structure.[8]

Synthetic peptides reproducing the N-terminal sequences of StII[12–15] and EqtII[16,17] have been used as an alternative experimental approach to clarify the contribution of the N-terminus segment to actinoporins action. In a previous paper,[12] we described the conformational and functional properties of the synthetic peptide $StII_{1–30}$ which contains the 1–30 N-terminal sequence of StII. This peptide exhibits hemolytic activity in the micromolar concentration range, being less active than the protein. However, $StII_{1–30}$ was found to form pores in red blood cells with radius ($\sim$ 1 nm) similar to that originated by the toxin and to acquire α-helical structure in membrane-mimetic systems, similar to that adopted by the equivalent sequence in the protein. Taken together, these results demonstrated that this synthetic peptide is a suitable model for studying the mechanism of pore formation by St II.[12]

Trp fluorescence is extremely sensitive to the polarity of the medium.[18] Therefore, the intrinsic fluorescence of Trp-containing peptides can be used to probe the microenvironment of this residue. To this end, we have synthesized four Trp-containing peptides (Trp-peptides: $StII_{1–30L2W}$, $StII_{1–30L12W}$, $StII_{1–30L17W}$, and $StII_{1–30L24W}$) where Leu residues 2, 12, 17, and 24, respectively were replaced by Trp in the $StII_{1–30}$ sequence (ALAGTIIAGASLTFQVLDKVLEELGKVSRK). To verify whether Trp substitutions had an effect on the main properties of the parent peptide, we have studied folding pattern in trifluorethanol (TFE), binding to lipid monolayers, and ability to permeabilize liposomes of Trp-peptides. Since Trp substitutions did not affect significantly the activity and conformation of the Trp-containing peptides, we examined their fluorescence properties in aqueous solution and in the presence of membranes. The results indicate that the Trp residues are inserted at different depths in the bilayer, demonstrating that $StII_{1–30}$ adopts an orientation with the N-terminus more deeply buried in the acyl chain region. This orientation reproduces the putative topology of this segment in the membrane-bound state of the full-length protein. Moreover, selective fluorescence quenching of Trp of $StII_{1–30L2W}$ by spin-labeled phosphatidylcholines suggests that the peptide's N-terminus is inserted in the bilayer interacting with positions located between the 5th and 12th C atoms of the acyl chains. Altogether, these results contribute to understand the orientation in the bilayer of $StII_{1–30}$, providing additional clues to the understanding of the mechanism of action of this peptide in membranes as a model of StII.

MATERIALS AND METHODS

Chemicals and Reagents

All 9-fluorenylmethyloxycarbonyl amino acids and Rink-amide MBHAR resin were purchased from Advanced Chemtech (Louisville, KY, USA) and Novabiochem (San Diego, CA, USA). Egg phosphatidylcholine (ePC), egg sphingomyelin (SM), 1-palmitoyl-2-oleoyl-sn-glycero-3-phosphate (POPA), and l-palmitoyl-2-(*n*-doxyl)-stearoyl-3-phosphatidylcholine (where $n = 5$, 12, and 16) (5-, 12-, 16-PCSL) were purchased from Avanti Polar Lipids (Alabaster, AL, USA). The lipids (99% pure) were used without further purification. Solvents and reagents were from Sigma–Aldrich Co (St. Louis, MO, USA) and Fluka (Buch, Switzerland).

Methods

Peptide Synthesis. The peptides, with amidated C-terminus, were synthesized manually according to the standard N_α-Fmoc protecting-group strategy[19] as previously described.[12] The peptides' homogeneity (>96% purity) was checked by reversed-phase analytical HPLC (Varian, Walnut Creek, CA, USA), using UV detection at 220 nm. The identity and molecular masses of the peptides were confirmed by electrospray mass spectrometry on a ZMD model apparatus (Micromass, Manchester, UK) and amino acid analysis (Shimadzu, Tokyo, Japan). $StII_{1–30}$ and Trp-containing peptides exhibited their expected molecular masses of 3129 Da and 3200 Da, respectively. Details on peptide quality control can be found in Supporting Information Figures S1, S2, and S3. Peptides were dissolved in deionized (MilliQ) water to render about 1 m*M* concentration that was quantitatively determined by a Micro BCA protein assay kit (Pierce, Illinois, USA) or using the Trp extinction coefficient at 280 nm (5690 $M\,cm^{-1}$).[20]

Surface Pressure Measurements on Lipid Monolayers. Surface pressure (π) measurements were carried out with a μThrough-S system (Kibron, Helsinki, Finland) at room temperature (22°C $\pm$ 2°C) under constant stirring employing plates of

about 3.14 cm^2. The aqueous phase consisted of 300 μL of Tris-buffered saline (TBS: 145 m*M* NaCl, 10 m*M* Tris–HCl, pH 7.4). The lipid mixture was pre-dissolved in chloroform:methanol (2:1, v:v) and was gently spread over the surface; the desired initial surface pressure (π_0) was attained by changing the amount of lipid applied to the air–water interface. The peptides were injected into the subphase to achieve 0.1 μM final concentration; at this concentration the peptides have no effect on surface tension of the air–water interface. The increment in surface pressure ($\Delta\pi$) was recorded as a function of the elapsed time until a stable signal was obtained.

Preparation of Lipid Vesicles. Films of ePC:SM:POPA (50:45:5) were prepared by evaporation of stock chloroform solutions using a stream of wet nitrogen and submitted to vacuum for not less than 2 h. For permeabilizing assays, multilamellar vesicles (MLV) were obtained by subsequent hydration in the presence of 80 m*M* carboxyfluorescein (CF), pH 7.4 (adjusted by adding NaOH) in water and subjected to six cycles of freezing and thawing. Large unilamellar vesicles (LUV) were prepared by extruding this MLV solution through a two-syringe LiposoFast Basic Unit extruder (Avestin Inc., Ontario, Canada) equipped with two stacked polycarbonate filters with 100 nm pore size (Nuclepore, Maidstone, UK). To remove untrapped fluorophore, vesicles were filtered through a mini-column (Pierce, Rockford, USA) loaded with Sephadex G-50 pre-equilibrated with TBS. To study binding to liposomes, small unilamellar vesicles (SUV) were prepared by sonication of a MLV suspension, prepared as described above, using an ultrasonicator (Branson 450, Danbury, USA) equipped with a titanium tip and subjected to 15 cycles of 2 min sonication with intervals of 1 min rest. Titanium particles released from the probe were removed by further centrifugation at 10,000*g* for 10 min at 22°C. Phospholipid concentration was measured by determining inorganic phosphate according to Rouser et al.[21] Lipid composition and concentration used are given in the text.

Assay of Leakage From Carboxyfluorescein-Containing Vesicles. LUV permeabilization was determined at room temperature (22°C ± 2°C) using a FLUOstar OPTIMA microplate reader (BMG Labtech, Offenburg, Germany) by measuring the fluorescence of released CF (λ_{exc} = 490 nm and λ_{em} = 520 nm). Black plastic 96-well microplates (SPL-Life Sciences, Seoul, South Korea) were pretreated with 0.1 mg/mL prionex (Pentapharm, Basel, Switzerland) which strongly reduces non-specific binding of protein and vesicles to plastic.[22] Peptide samples (up to 5 μ*M* final concentration) were twofold serially diluted in the well microplates in a final volume of 100 μL of TBS and the reaction was started by adding the same volume of liposomes (10 μ*M* final lipid concentration).

After mixing vesicles and peptides, the release of CF into the external medium produced an increase in fluorescence (f), due to dequenching of the dye's fluorescence resulting from dilution. The increase in fluorescence was recorded as a function of time. Maximum release was obtained by adding 0.1% Triton X-100 (final concentration) and provided the fluorescence value f_{max}. The fraction of released fluorophore (F) was calculated as follows:

$$F = (f_t - f_o)/(f_{max} - f_o) \quad (1)$$

where f_o and f_t represent the values of fluorescence in the absence or the presence (at time t) of peptides, respectively.

Hemolytic Activity. Hemolytic activity was evaluated turbidimetrically at 600 nm at room temperature (22°C ± 2°C) in a Lab systems microplate reader (Helsinki, Finland) as previously described.[12] Erythrocyte suspension was prepared using pooled fresh human red blood cells collected intravenously from at least four healthy volunteers. Cells were washed by repeated centrifugation (600*g*, 15 min), the cell pellet resuspended in TBS and finally diluted to an apparent absorbance of 0.1 at 600 nm. Peptide samples in 100 μL of TBS were twofold serially diluted (up to 40 μ*M* final concentration) in a flat-bottom 96-well microplate. The reaction was started by adding the same volume of red blood cells (200 μL total volume). The decrease in apparent absorbance was recorded as a function of time with intermittent shaking. The hemolytic activity (HA) was calculated as follows:

$$HA = (OD_0 - OD_t)/(OD_0 - OD_{min}) \quad (2)$$

where OD_t, OD_0, and OD_{min} represent the apparent absorbance at time t, at time zero, and in the presence of an excess of peptide, respectively.

Pore Size Determination. Pore size was determined in human red blood cells following the hemolytic assay described in the previous section. Briefly, in each well, a fixed concentration (10 or 160 μ*M*) of StII$_{1-30}$ or StII$_{1-30L2W}$ was present, in a final volume of 100 μL of TBS, with or without 60 m*M* of one member of the polyethylene glycol series (with their hydrated radii in parentheses): PEG200 (0.40 nm), PEG400 (0.56 nm), PEG600 (0.69 nm), PEG900 (0.85 nm), PEG1000 (0.89 nm), PEG1500 (1.1 nm), PEG2000 (1.27 nm), and PEG3000 (1.4 nm). Addition of large osmoticants increased the half-time of peptide–induced hemolysis (t1/2), in a size-dependent manner. The difference $t1/2 - t1/2^\circ$, the half-times in the presence and absence of osmotic protectants, respectively, was used as an estimate of the induced delay. This parameter measures the time necessary for an osmolite to diffuse inside the cell through the toxin-induced lesions. Accordingly, $1/(t1/2 - t1/2^\circ)$ is an estimate of the PEG permeability through the pore, which is inversely related to the PEG size. Thus, dividing the data by the permeability of a reference polymer (in this case, PEG200) the dependence of the relative permeability of the molecules versus their size was fitted to a Renkin plot[23]; which allowed estimating the radii of the pores formed by both peptides.

Circular Dichroism Studies. Circular dichroism (CD) spectra were acquired in 0.5 mm path length cuvettes, at room temperature (22°C ± 2°C) using a Jobin Yvon CD6 spectropolarimeter (Jobin Yvon, Longjumeau, France). The instrument was routinely calibrated with an aqueous solution of recrystallized D-10-camphorsulfonic acid. Samples were prepared by mixing appropriate amounts of two peptide stock solutions (10 μ*M*), one in 100% TFE and the other in MilliQ water adjusted to pH 7.4.

Fluorescence Assays with Trp-Containing Peptides Analogs of StII$_{1-30}$. Binding of Trp-peptides to SUV was followed by the increase in Trp fluorescence. For this study, SUV were selected instead of LUV in order to avoid spectra distortion due to light scattering. Fluorescence measurements were carried out at room temperature (22°C ± 2°C) in a spectrofluorimeter (Hitachi, F-4500, Tokyo, Japan) using quartz cuvettes with excitation and emission slits of 5 and 10 nm, respectively. The samples were excited at 280 nm

and the emission spectra were recorded from 300 to 440 nm. Increasing amounts of SUV were added to the peptide in milliQ water adjusted to pH 7.4, and the spectrum was recorded for each lipidic concentration. Corrections were made for sample dilution and for light scattering caused by the vesicles.

Quenching of Trp Intrinsic Fluorescence by Acrylamide. Quenching of Trp was achieved by adding the water-soluble quencher acrylamide in the presence of SUV. Acrylamide quenching experiments were carried out using 20 μM of peptide and 400 μM of total lipid. Samples were prepared in MilliQ water adjusted to pH 7.4; excited at 280 nm and the emission spectra were recorded from 300 to 440 nm after addition of acrylamide (up to 0.25 mM). Spectral correction was made by subtracting spectra measured under identical conditions but without the peptide. The maximum fluorescence intensities without and with the quencher (F_{AA0} and F_{AA}, respectively) were determined and F_{AA0}/F_{AA} values were plotted as a function of acrylamide concentration (Q). The experimental data were analyzed according to the Stern–Volmer equation:.

$$F_{AA0}/F_{AA} = 1 + K_{sv}[Q] \quad (3)$$

The slopes of the best-fit linear plots were used to determine the Stern–Volmer quenching constants (K_{SV}).[18]

Quenching of Trp Intrinsic Fluorescence by Spin-Labeled PCs. SUV of ePC:SM:POPA (25:45:5) were prepared containing additional 25 mole% of the lipid-soluble spin-labeled phosphatidylcholines (PCSL) carrying the nitroxide moiety at carbons 5 (5-PCSL), 12 (12-PCSL), or 16 (16-PCSL) on the *sn*-2 stearoyl chain.[24] Experiments were carried out using 20 μM of peptide and 400 μM of total lipids. Samples were prepared in MilliQ water adjusted to pH 7.4; excited at 280 nm and the emission spectra were recorded from 300 to 440 nm. Spectral correction was made by subtracting the spectra measured under identical conditions but without the peptide. Fluorescence intensity of $StII_{1-30L2W}$ was recorded and quenching reported as the peptide remaning maximal fluorescence (%):

$$R(\%) = (f_L)/(f_{nL}) \times 100 \quad (4)$$

where f_L is the fluorescence of the peptide in the presence of spin-labeled vesicles and f_{nL} is the peptide fluorescence in the presence of non-labeled vesicles. The actual spin probe concentration (~ 100 μM) in the vesicle preparation was determined from the electron paramagnetic resonance spectrum using tempol (2,2,6,6-tetramethyl-4-hydroxy-*N*-oxylpiperidine) as a standard.

RESULTS

Functional and Conformational Properties of the Trp-Containing Peptides

To determine the orientation of $StII_{1-30}$ in membrane, we synthetized four Trp-containing peptides in which a Leu residue corresponding to position 2 ($StII_{1-30L2W}$), 12 ($StII_{1-30L12W}$), 17 ($StII_{1-30L17W}$), or 24 ($StII_{1-30L24W}$) was replaced by Trp, an aromatic residue often used in fluorescent studies of peptides and proteins.[25,26] The substitutions cover the entire length of $StII_{1-30}$ and are located at different positions corresponding to a hydrophobic segment (1–10) or the nonpolar face of the amphipatic α-helix described by Mancheño et al. for StII[4] (Figure 1). Thus, it was necesary to verify whether the Trp analogs of $StII_{1-30}$ conserved the native peptide functional properties. For this purpose, binding of the peptides to monolayers was examined, as well as their permeabilization of LUV. Lipid monolayers and LUV were composed of ePC and SM in almost equimolar proportion, since this binary composition has proven to be adequate to study the binding of sticholysins to lipid membranes.[27] A small proportion of the anionic phospholipid POPA was also included (ePC:SM:POPA, 50:45:5), since its presence significantly favours $StII_{1-30}$-membrane interaction.[15] This phospholipid is present only in small amount in the outer layer of the cell membrane,[28,29] thus including 5 mole% into the lipid mixture could be mimicking the cell composition of mammalian cells.

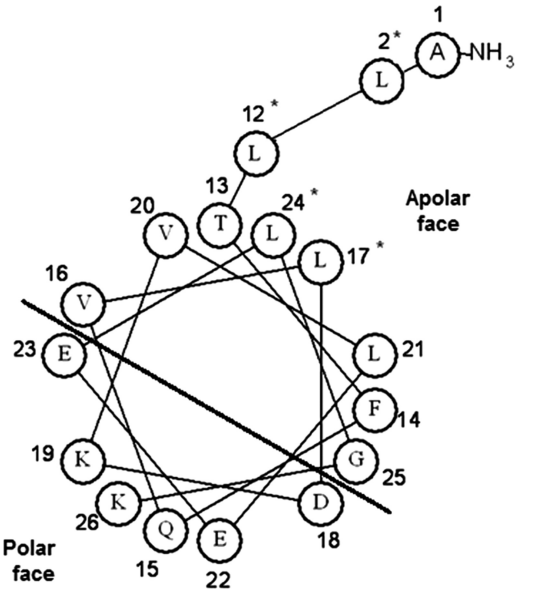

FIGURE 1 Hydrophobic stretch and amphipatic α-helix wheel projection of $StII_{1-30}$. The StII hydrophobic stretch and the α-helix include the 1-10 and 14-23 amino acid sequences, respectively. Leu residues substituted by Trp in the analog peptides are marked with an asterisk.

The increase in lipid monolayer surface pressure ($\Delta\pi$) prompted by binding of the peptides was examined at several initial pressures (π_o) at constant area to describe their ability to interact with organized lipids (Figure 2). The inset to the figure shows a typical time-course of the surface pressure increase arising from peptide binding (π_0 =20 mN · m^{-1}). A suitable parameter for the characterization of peptide-lipid interaction is the critical pressure (π_c), which corresponds to

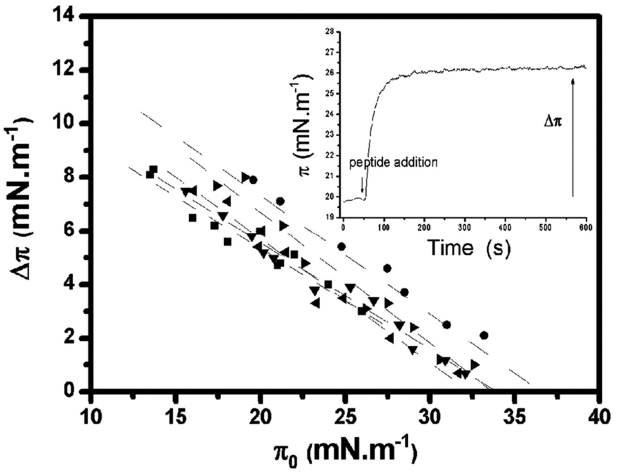

FIGURE 2 Increase in surface pressure induced by the peptides as a function of initial monolayer pressure. $\Delta\pi$ is the pressure increase of the lipid monolayer due to peptide binding. Inset: Time-course of StII$_{1-30}$ insertion in the lipid monolayer characterized by $\pi o = 20$ mM.m^{-1}. Peptide concentration: 0.1 μM. Lipid composition: ePC:SM:POPA (50:45:5). TBS buffer, pH 7.4, T 22 ± 2°C. StII$_{1-30}$ (■), StII$_{1-30L2W}$ (●), StII$_{1-30L12W}$ (▼), StII$_{1-30L17W}$ (◀), StII$_{1-30L24W}$ (▶).

the pressure that must be applied to avoid incorporation of the peptides into the monolayer and is directly correlated with their affinity for the lipids.[30] This value is almost identical for all peptides ($\sim$ 34 mN · m^{-1}) except for StII$_{1-30L2W}$, which is distinguished by a relatively higher affinity ($\pi_o \sim 37$ mN · m^{-1}) (Table I).

The addition of the peptides to lipid vesicles containing entrapped CF allowed assessing their permeabilizing activity by following the release of the fluorophore as a function of time. If a single pore in a vesicle is enough to instantaneously lead to total leakage of the fluorophore,[31] the final extent of fluorescence increase elicited by the peptide can be related to the fraction of vesicles in which at least one pore has been formed (F). As illustrated for StII$_{1-30L2W}$ in Figure 3, addition of all Trp-containing peptides induced permeabilization of the vesicles. Similarly to what was observed for StII$_{1-30}$, the effect was both time- and dose-dependent.[15] The activity of all Trp-containing peptides occurs in the micromolar range, as demonstrated for StII$_{1-30}$[15] and for most membranolytic peptides.[32] To compare the activity of StII$_{1-30}$ and Trp-containing peptides, the extent of permeabilization after 30 min (F_{30min}) was calculated (Table I). According to F_{30min}, all the peptides (at a concentration of 5 μM) promote the permeabilization of about 0.8 fraction of vesicles, taking as maximal fraction the signal obtained with Triton X-100. The evidence that apparently not all vesicles are permeabilized could be related to the fact that Triton X-100 affects the fluorescence of CF either directly[33] or indirectly, diminishing light scattering by disruption of membrane integrity, as previously demonstrated for StII$_{1-30}$.[15]

Since StII exhibits hemolytic activity, we decided to test the ability of the peptides to promote human red blood cell lysis. Figure 4A shows the time course of StII$_{1-30L2W}$–elicited hemolysis. As in vesicle permeabilization assays, all the peptides promote erythrocytes lysis. The activity of all peptides occurs in the micromolar concentration range and is dose-dependent as previously described for StII$_{1-30}$.[12,13] All the peptides (40 μM) cause the lysis of almost all the erythrocytes, similarly to the positive control with an excess of peptide (Table I). Additionally, we decided to estimate the size of the lesion caused by StII$_{1-30L2W}$ in the cell membrane, taking advantage of the colloid–osmotic characteristics of peptide-induced hemolysis. The method was essentially the same as previously described to estimate the radii of the pores formed by StII[34] and StII$_{1-30}$[15] by fitting the data in Figure 4B to a Renkin plot.[23] This provided an estimate for the pore radii of

Table I Parameters Derived from Binding to Monolayers, LUV Permeabilization, Hemolytic Activity, and CD Spectra of Peptides

Peptide	$\pi_c \pm$ SD (mN m^{-1})	$F_{30\ min} \pm$ SD	HA$_{30\ min} \pm$ SD	α-helix[a] (# of aminoacids)	$\theta_{222}/\theta_{208}$[a]
StII$_{1-30}$	33.7 ± 1.1	0.81 ± 0.04	1.0 ± 0.02	15	0.86
StII$_{1-30L2W}$	37.5 ± 0.5	0.84 ± 0.02	1.0 ± 0.02	16	0.91
StII$_{1-30L12W}$	33.9 ± 0.5	0.79 ± 0.02	1.0 ± 0.01	15	0.84
StII$_{1-30L17W}$	32.4 ± 0.7	0.78 ± 0.06	0.9 ± 0.8	17	0.87
StII$_{1-30L24W}$	34.1 ± 0.7	0.77 ± 0.04	1.0 ± 0.02	14	0.80

π_c: Pressure that must be applied to avoid incorporation of the peptide to the monolayer. This parameter indicates the affinity of the peptides for the lipid ensemble and is calculated by extrapolating regression lines from plots of $\Delta\pi$ vs. π_o (Figure 2) ($r^2 > 0.94$). F_{30min}: Extension of LUV permeabilization after 30 min of peptide addition. Values represent the fraction of permeabilized vesicles, taking as maximal reference (1.0) the signal obtained in the presence of Triton X-100. HA$_{30min}$: Extension of the hemolysis in red blood cells induced after 30 min of peptide addition. The values represent the fraction of permeabilized cells, taking as maximal reference (1.0) the signal obtained in the presence of an excess of peptide. Experiments were done in triplicate and each value represents the mean ± the standard deviation (SD). [a] Calculated from CD spectra in the presence of TFE (60%) according to Chen et al.[45] Peptide concentration: monolayer experiments, 0.1 μM; permeabilization assay, 5 μM; hemolytic assay, 40 μM; and CD studies, 10 μM.

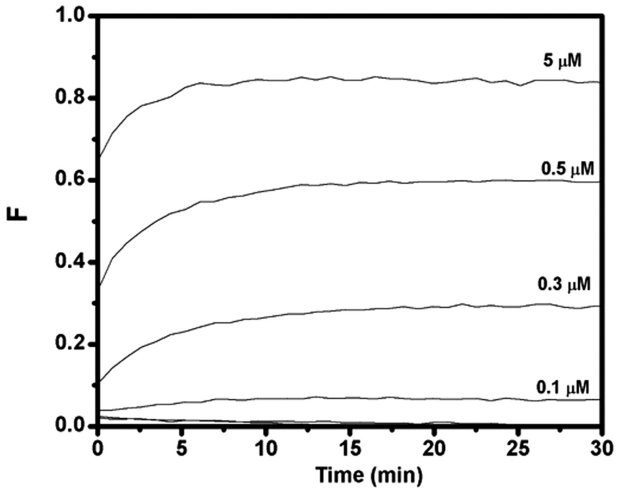

FIGURE 3 Time course of LUV permeabilization induced by $StII_{1-30L2W}$. F represents the fraction of vesicles that contain at least one channel. Lipid concentration: 10 μM. Lipid composition: ePC:SM:POPA (50:45:5). TBS buffer, pH 7.4, T 22 ± 2 °C.

about 1.1 nm for $StII_{1-30}$ and 1.3 nm for $StII_{1-30L2W}$. The radius of the pore herein estimated is consistent with the value (~1 nm) reported for $StII_{1-30}$ by Casallanovo et al.[12]

Peptides folding (10 μM) was also explored by CD spectroscopy in the presence of ePC:SM:POPA (50:45:5) SUV at a total lipid concentration below 300 μM. Nevertheless, the interpretation of the results was not straightforward in view of light scattering due to the high SM content of the vesicles. Thus, in order to gain insight into the conformation acquired by Trp-containing peptides in a system that mimics the hydrophobic properties of membranes, their secondary structure was studied by far-UV CD in TFE and compared with that of $StII_{1-30}$. Far-UV CD spectra of the peptides were obtained in the presence of 60% TFE. All spectra exhibit a positive band around 195 nm, and minima centered at 208 and 222 nm; features that are ascribed to α-helical conformation.[35] The differences in the number of amino acids in α-helical structure among the peptides are not relevant (less than three amino acid residues, which corresponds to less than one α-helical turn) (Table I). In addition, the ratio between the negative bands at 222 and 208 nm ($[\theta_{222}]/[\theta_{208}]$) is about 0.8, reflecting that the peptides adopt typical monomeric α-helical conformation in TFE.[36]

Binding of Trp-Containing Peptides to Lipid Vesicles

Trp fluorescence is a useful tool to study binding of proteins and peptides to membranes by sensing changes in their local environment. Here, Trp-analogs of $StII_{1-30}$ were used to determine their orientation in SUV as membrane mimetic systems. For this purpose, peptide-lipid interactions were monitored by following the changes in Trp fluorescence emission spectra of the peptides upon addition of SUV. Additionally, it was determined the differential quenching of Trp fluorescence caused by either acrylamide or PCSL, as water- or lipid-soluble quenchers, respectively.

F/F_0 ratios calculated from the spectra of Trp-containing peptides plotted *vs.* lipid concentration show an increase in fluorescence intensity until saturation, giving rise to binding isotherms (Figure 5A). For $StII_{1-30L2W}$ and $StII_{1-30L12W}$, the fluorescence increase at saturation is around threefold and twofold, respectively; in contrast with $StII_{1-30L17W}$ and $StII_{1-30L24W}$ for which the fluorescence emission barely

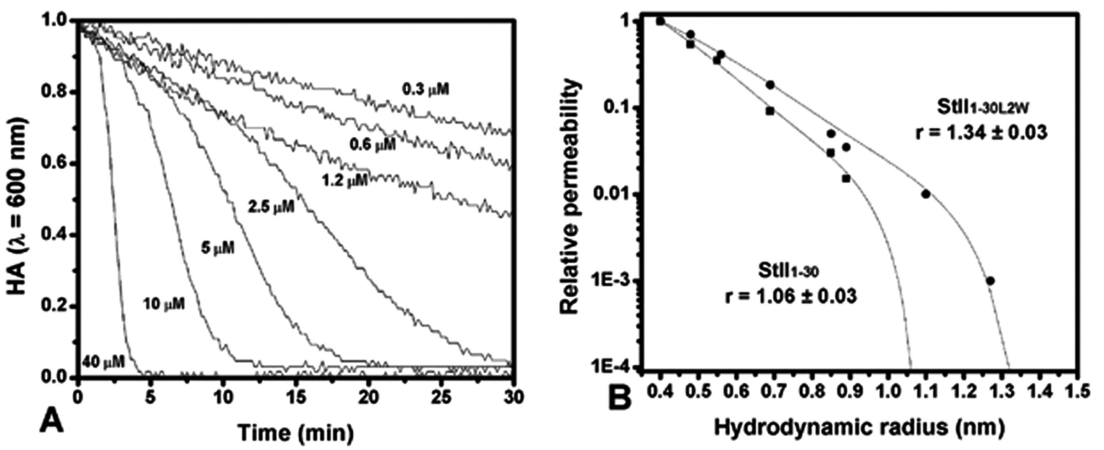

FIGURE 4 Hemolytic activity and size of the pore elicited in red blood cells by $StII_{1-30L2W}$. A) Time course of hemolysis as a function of peptide concentration. HA represents the fraction of cell lysis. B) Radius of the pore formed by $StII_{1-30}$ (■) and $StII_{1-30L2W}$ (●) estimated from the Renkin plot.[23] The solid lines are best fits of the Renkin equation for all experimental values obtained. r is the radius size. $R^2 = 0.99$. TBS buffer, pH 7.4, T 22 ± 2°C.

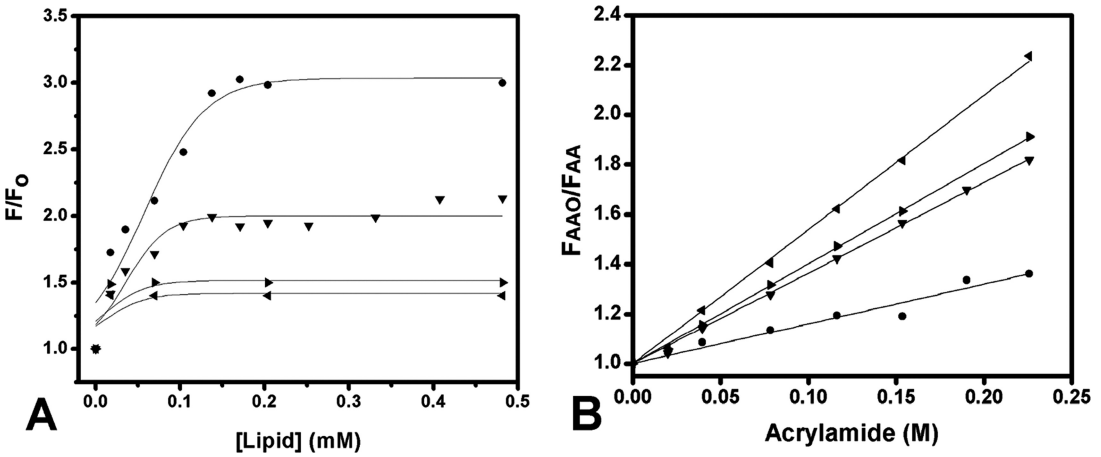

FIGURE 5 Fluorescence studies of Trp-containing peptides analogs of StII$_{1-30}$ in the presence of SUV. A) Increase of fluorescence intensity as a function of lipid concentration. F_0 and F stand for the fluorescence intensities (at λ_{max}) in the peptides spectra in the absence and presence of SUV, respectively. B) Stern–Volmer plots for acrylamide quenching of the peptides' Trp fluorescence in the presence of 400 μM total lipid. Fluorescence intensities, measured in the absence (F_{AA0}) and presence (F_{AA}) of vesicles are plotted according to the Stern–Volmer equation ($r^2 > 0.96$). λ_{exc} = 280 nm, λ_{em} = 310–440 nm; T 22 ± 2°C. Peptide 20 μM and ePC:SM:POPA (50:45:5) SUV in water adjusted to pH 7.4. StII$_{1-30L2W}$ (●), StII$_{1-30L12W}$ (▼), StII$_{1-30L17W}$ (◀), StII$_{1-30L24W}$ (▶).

increases about 1.5-fold. Selective quenching of the fluorescence emitted by Trp moieties located in different microenvironments was achieved by adding increasing concentrations of acrylamide.[18] The studies with the water-soluble quencher were carried out in the presence of saturating lipid concentrations in order to ensure that essentially all peptide molecules were bound to liposomes. The calculation of Stern-Volmer constants (K_{sv}) from the slopes in Figure 5B allowed estimating the quenching efficiency. The values of λ_{max}, obtained from typical fluorescence spectra of peptides, and K_{sv} values, obtained in the presence of liposomes (Figure 6A) shows that Trp fluorescence of the peptides behave dif-

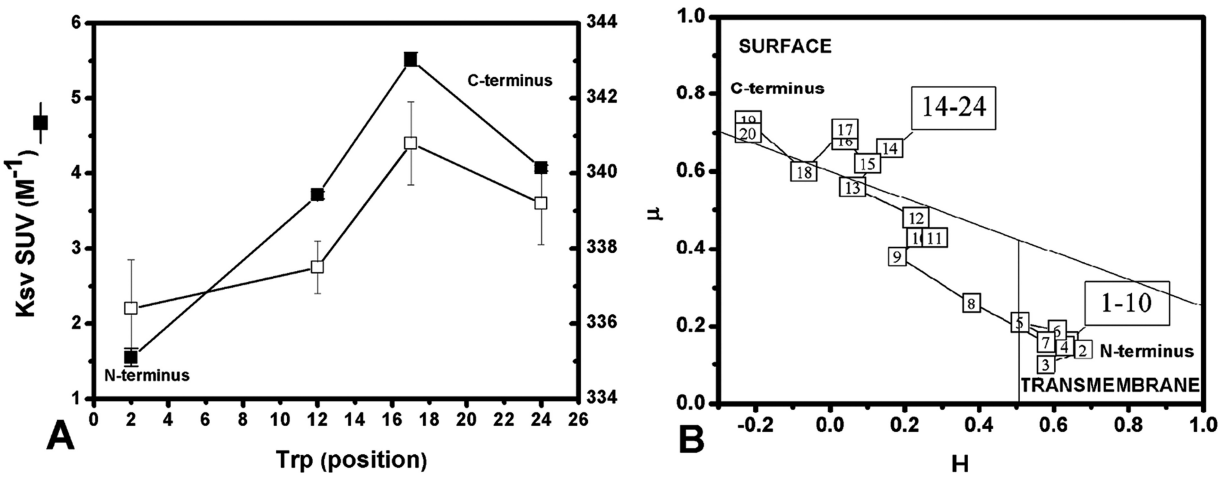

FIGURE 6 StII$_{1-30}$ orientation in membrane. A) Values of K_{sv} and λ_{max} obtained from the fluorescence data in Figure 5. B) Prediction of peptide orientation using the hydrophobic moment plot. H represents the mean hydrophobicity and μ the mean hydrophobic moment. The diagram was built according to the Eisenberg procedure and includes segment classification (surface and transmembrane) boundaries[37] Each data point represents an 11-residue segment of StII$_{1-30}$. The number indicates the first amino acid of the segment, according to the StII$_{1-30}$ sequence. The hydrophobic stretch (1–10) and the amphiphilic α-helix segment (14–24) from StII's 3D structure[4] are pointed out. The profiles obtained for Trp-containing peptides are identical to those shown for StII$_{1-30}$ and, consequently, are not shown in the figure.

ferently upon binding to membranes. While the spectra of $StII_{1–30L2W}$ and $StII_{1–30L12W}$ exhibit the lowest λ_{max} (336 nm and 337 nm, respectively), these values are 341 nm and 339 nm for the spectra of $StII_{1–30L17W}$ and $StII_{1–30L24W}$, respectively. In agreement with these observations, $StII_{1–30L2W}$ exhibits the lowest K_{sv} value for acrylamide quenching, followed by $StII_{1–30L12W}$.

Putative transmembrane α-helical segments of proteins or peptides can be predicted, based on the hydrophobic moment plot.[37] To this end, we assumed that both the hydrophobic stretch (1–10) and the amphipathic segment (14–23) of $StII_{1–30}$ and the Trp-analog peptides were folded in α-helical conformation. This hypothesis is supported by the fact that all the peptides adopt in TFE a longer α-helix (Table I) than the corresponding in the StII crystal structure[4] as previously demonstrated by Casallanovo et al.[12] for $StII_{1–30}$. In this paper, we suggested that the hydrophobic sequence in the N-terminal region (1–10) enhances the propensity of $StII_{1–30}$ to adopt helical conformation even though we could not define whether residues to the C-terminal portion also participate in the lengthening of the helix. However, studies on the structure of a peptide derived from the N-terminus of StI ($StI_{1–30}$) in 30% TFE by NMR have provided further evidence of the hydrophobic stretch ability to adopt helical structure in a membrane mimetic system. In fact, the peptide forms a helix-turn-helix motif with the two α-helices spanning residues 4–9 or 12–28, respectively.[14] Therefore, it is conceivable that this motif is also present in $StII_{1–30}$ and Trp-containing analogs.

Figure 6B shows the mean hydrophobic moment (μ)—a measure of the amphipathicity—as a function of the corresponding mean hydrophobicity (H). These properties were calculated over a sliding window of eleven amino acid residues from $StII_{1–30}$'s N-terminus and the resulting 11-amino acid segments were identified with the number of the first amino acid of that segment. Analysis of the Eisenberg plot reveals that the peptide seems to adopt an oblique orientation in membrane since the hydrophobic stretch (included in the segment 1–11) has a propensity to adopt a transmembrane orientation while the amphipathic α-helix (comprising the 14–24 segment) has a tendency to lie at the membrane interface being predicted as a surface seeking stretch. It is noteworthy that Trp substitutions did not modify this putative orientation of $StII_{1–30}$.

In order to get further insight into the depth of penetration of $StII_{1–30}$'s N-terminus in the bilayer, fluorescence quenching experiments using lipid soluble spin-labeled PCs carrying the spin label moiety at different carbons along the *sn-2* stearoyl fatty acyl chain (5-, 12-, or 16-PCSL) were carried out with $StII_{1–30L2W}$. In this assay, the spin label in 5-PCSL was located closer to the bilayer-water interface, while in 12- and 16-PCSL the nitroxide moiety was located closer to the terminal methyl groups in the hydrophobic core of the membrane. Thus, selective fluorescence quenching by the spin labels could provide an indication of the depth of Trp location in the bilayer.[24] It was observed that the extent of fluorescence quenching in systems containing spin-labeled PCs depends on the probe position, *i.e.*, the fluorescence of Trp at position 2 of the vesicle-bound peptide ($StII_{1–30L2W}$) was reduced by about 17% by 5-PCSL and about 30% by 12-PCSL. In contrast, the quenching effect of 16-PCSL was almost negligible ($\sim$ 2%).

DISCUSSION

StII is the most potent pore-forming toxin produced by the sea anemone *Sticholdactyla helianthus*.[31] The first thirty N-terminal amino acid residues are thought to be the best candidates for pore formation. This region contains an amphipathic stretch, where residues 14–23 were seen to form an amphipathic α-helix in the crystal structure.[4] This sequence is well conserved in all actinoporins[38] and is clearly similar to some membrane-interacting peptides such as melittin and fusogenic viral peptides.[33,39,40] In previous works we demonstrated that peptides reproducing sticholysins N-termini can mimic the permeabilizing ability of the toxins.[12,15] In particular, the peptide derived from StII ($StII_{1–30}$) was the most active, becoming the best candidate to obtain insight into its molecular mechanism of action and, by extension, that of sticholysins.[15]

In this work, we synthesized four Trp-substituted analogs of $StII_{1–30}$ to estimate the peptide's orientation based on the fluorescence properties of Trp. For this purpose, we used the strategy of replacing Leu by Trp in positions 2 ($StII_{1–30L2W}$), 12 ($StII_{1–30L12W}$), 17 ($StII_{1–30L17W}$), or 24 ($StII_{1–30L24W}$). Since these residues are located in different positions along the peptide sequence, this study allowed exploring the effect of the microenvironment on their fluorescence properties, rendering possible to estimate the topology of $StII_{1–30}$ in the bilayer. To validate the use of Trp-substituted peptides as models of $StII_{1–30}$, experiments were carried out to compare their properties with those of the parent peptide. Specifically, we investigated peptide binding to lipid monolayers, their ability to permeabilize liposomes, and their conformation in TFE, as a membrane mimetic environment. Trp substitution did not modify the properties of the peptides significantly. In fact, all Trp-peptides are able to promote complete lysis of human red blood cells and to permeabilize lipid vesicles (Table I) in the micromolar concentration range, reproducing the activity profile of $StII_{1–30}$. Additionally, all peptides bind

to lipid monolayers with similar affinity and predominantly adopt analogos α-helical conformation in TFE (Table I), as previously described for StII$_{1-30}$.[12,15]

Fluorescence studies permitted sensing differences in the polarity of the local environments surrounding Trp in the vesicle-bound peptides. It is well known that the transfer of Trp residues from the polar aqueous phase to the less polar membranous environment causes a blue-shift of the emission spectra, as well as an increase in fluorescence intensity.[18] The F/F_0 ratio at saturating lipid concentrations indicates that the Trp residues located at different positions in StII$_{1-30}$ fluorescent analogs are located in different micro-environments. In particular, the fact that the values of F/F_0 for the spectra of StII$_{1-30L17W}$ and StII$_{1-30L24W}$ are close to 1.0 supports the idea that residues 17 and 24 are associated with, but not deeply inserted into the bilayer. In contrast, the higher F/F_0 values for the spectra of StII$_{1-30L2W}$ and StII$_{1-30L12W}$ indicate a greater depth of insertion of residues 2 and 12. Moreover, the smaller values of λ_{max} and K_{sv} obtained for StII$_{1-30L2W}$ evinces that Trp^2 is most deeply buried into the membrane (Figure 6A). Conversely, Trp residues in StII$_{1-30L12W}$, StII$_{1-30L17W}$, and StII$_{1-30L24W}$ are more exposed to the water-lipid interface as shown by the higher values of λ_{max} and K_{sv}. This piece of evidence supports the idea that StII$_{1-30}$ is oriented in bilayers with the N-terminus in the direction of the membrane hydrophobic core and the C-terminus towards the water-lipid interface (Figure 6).

In order to obtain an approximation of the localization of StII$_{1-30}$ α-helix in the bilayer, we measured the quenching of StII$_{1-30L2W}$'s fluorescence by spin-labeled PCs incorporated in SUV. This peptide was selected taking into account that Trp^2 seems to be the most deeply inserted into the bilayer. Additionally, we experimentally determined that StII$_{1-30L2W}$ is able to form pores whose size is similar to those formed by StII$_{1-30}$ (Figure 4B). The data obtained in the presence of the lipid-soluble quenchers revealed that peptide's N-terminus interacts with the fatty acyl chain located between positions 5 and 12. Therefore, given that the C-C distance of a single bond in the acyl chain is 1.54 Å and that in the all-*trans* conformation, the bond angle is 109°, each C-C bond contributes 1.25 Å to the length of the chain. Consequently, taking carbon 12 of the acyl chain as a reference, the depth of the peptide α-helix in the bilayer would be approximately 14 Å. As a result, if we assume that each residue in an α-helix increases the helix length in about 1.5 Å, it could be reasonably estimated that about nine residues of the peptide's N-terminus would be inserted into the membrane. This calculation is in agreement with our prediction results based on the classical Eisenberg plot.[37] Such prediction envisages that StII$_{1-30}$ could adopt an oblique orientation in the membrane, with the hydrophobic stretch 1–10 in contact with the hydrophobic core and the amphiphilic sequence 14-24 lying at the water-lipid interface (Figure 6B).

Particularly, this result clearly suggests that StII$_{1-30}$ does not span the full bilayer thickness, since Trp^2 does not seem to be close to carbon 16 of the hydrophobic lipid tails; similarly as previously found for sticholysins.[10] Making use of differential scanning calorimetry, we have found that StII$_{1-30}$ raises the bilayer to hexagonal phase transition temperature of dipalmitoleoylphosphatidylethanolamine by about 3°C (unpublished results), suggesting that the peptide is able to induce positive curvature in membranes. This is in line with the toroidal pore model proposed for the mechanism of action of actinoporins,[4,10,11] as well as of a large number of membranotropic peptides, such as magainin.[41,42] In this model, the phospholipid head group region preferentially interact with the polypeptide backbone and the pore is formed by membrane lipids in conjunction with peptide or protein α-helices.[43] It has been hypothesized that membranolytic proteins could generate membrane deformation by partially inserting into the bilayer.[44] Accordingly, if we take into account the predicted ability of the hydrophobic stretch containing residues 1–10 to interact with the hydrophobic membrane core, it is reasonable to assume that the insertion of this segment into the membrane would promote lipid reorganization and the establishment of the pore architecture.

In conclusion, the present results provide further evidence regarding the ability of a peptide derived from the N-terminal sequence of StII to mimic the function of this toxin. Similarly to the whole protein, StII$_{1-30}$ exerts both hemolytic and permeabilizing activity in vesicles. Red blood cell lysis, and probably vesicle permeabilization as well, are the result of formation of a pore of around 1 nm radius by the peptide, similar to that described for StII.[34] Here, it was demonstrated that membrane permeabilization is associated to the peptide ability to adopt a membrane topology with the N-terminus oriented in the direction of the bilayer core and the C-terminus towards the lipid-water interface, similar to that proposed for this segment of StII during pore formation.[4] In this topology, StII$_{1-30}$ does not seem to interact with the carbons in the phospholipid acyl chains located closer to the core of the membrane, probably due to the fact that only the stretch containing residues 1-10 appears to be deeply buried in the bilayer. Further studies should be carried out aiming at elucidating whether this peptide promotes lipid reorganization leading to a pore structure with toroidal architecture.

REFERENCES

1. Lanio, M. E.; Morera, V.; Alvarez, C.; Tejuca, M.; Gomez, T.; Pazos, F.; Besada, V.; Martinez, D.; Huerta, V.; Padron, G.; Chavez, M. A. Toxicon 2001, 39, 187–194.

2. Kem, W. R. In The Biology of Nematocysts; Academic Press: San Diego, 1988.
3. Anderluh, G.; Macek, P. Toxicon 2002, 40, 111–124.
4. Mancheño, J. M.; Martin-Benito, J.; Martínez-Ripoll, M.; Gavilanes, J. G.; Hermoso, J. A. Structure 2003, 11, 1319–1328.
5. Castrillo, I.; Alegre-Cebollada, J.; del Pozo, A. M.; Gavilanes, J. G.; Santoro, J.; Bruix, M. Biomol NMR Assign 2009, 3, 5–7.
6. Athanasiadis, A.; Anderluh, G.; Macek, P.; Turk, D. Structure 2001, 9, 341–346.
7. Hinds, M. G.; Zhang, W.; Anderluh, G.; Hansen, P. E.; Norton, R. S. J Mol Biol 2002, 315, 1219–1229.
8. Mechaly, A. E; Bellomio, A.; Gil-Cartón, D.; Morante, K.; Valle, M.; González-Mañas, J. M.; Guérin, M. A. Structure 2011, 19, 181–191.
9. Alvarez-Valcárcel, C.; Dalla Serra, M.; Potrich, C.; Bernhat, I.; Tejuca, M.; Martínez, D.; Pazos, F.; Lanio, M. E.; Martínez, D.; Menestrina, G. Biophys J 2001, 80, 2761–2774.
10. Alvarez, C.; Casallanovo, F.; Shida, C. S.; Nogueira, L. V.; Martínez, D.; Tejuca, M.; Pazos, I. F.; Lanio, M. E.; Menestrina, G.; Lissi, E.; Schreier, S. Chem Phys Lipids 2003, 122, 97–105.
11. Anderluh, G.; Dalla-Serra, M.; Viero, V.; Guella, G.; Macek, P.; Menestrina, G. J Biol Chem 2003, 278, 45216–45223.
12. Casallanovo, F.; de Oliveira, F. J.; de Souza, F. C.; Ros, U.; Martinez, Y.; Pentón, D.; Tejuca, M.; Martínez, D.; Pazos, F.; Pertinhez, T. A.; Spisni, A.; Cilli, E. M.; Lanio, M. E.; Alvarez, C.; Schreier, S. Biopolymers 2006, 84, 169–180.
13. Cilli, E. M.; Pigossi, F. T.; Crusca, E.; Ros, U.; Martínez, D.; Lanio, M. E.; Alvarez, C.; Schreier, S. Toxicon 2007, 50, 1201–1204.
14. Castrillo, I.; Araujo, N. A.; Alegre-Cebollada, J.; Gavilanes, J.; Martínez-del-Pozo, A.; Bruix, M. Proteins 2010, 78, 1959–1970.
15. Ros, U.; Pedrera, L.; Diaz, D.; de Karam, J. C.; Sundbrack, T. P; Valiente, P. A.; Martínez, D.; Cilli, E. M.; Pazos, F.; Itri, R.; Lanio, M. E.; Schreier, S.; Alvarez, C. J Biosci 2011, 36, 781–791.
16. Drechsler, A.; Potrich, C.; Sabo, J. K.; Frisanco, M.; Guella, G.; Dalla Serra, M.; Anderluh, G.; Separovic, F.; Norton, R. S. Biochemistry 2006, 45, 1818–1828.
17. Drechsler, A.; Miles, A.; Norton, R. S.; Wallace, B. A.; Separovic, F. Eur Biophys J 2009, 45, 1818–1828.
18. Lakowicz, J. R. Principles of Fluorescence Spectroscopy,3rd ed.; Springer, New York, 2006.
19. Atherton, E.; Sheppard, R. C. Solid Phase Peptide Synthesis: A Practical Approach; Oxford University Press: Oxford, 1989.
20. Gill, S. C.; von Hippel, P. H. Anal Biochem 1989, 182, 319–326.
21. Rouser, G.; Fleischer, S.; Yamamoto, A. Lipids 1970, 5, 494–496.
22. Dalla Serra, M.; Fagiuoli, G.; Nordera, P.; Bernhart, I.; Della Volpe, C.; Di Giorgio, D.; Ballio, A.; Menestrina, G. Mol Plant Microbe Interact 1999, 12, 391–400.
23. Renkin, E. M. J. Gen Physiol 1954, 38, 225–243.
24. Chattopadhyay, A.; London, E. Biochemistry 1987, 26, 39–45.
25. Matsuzaki, K.; Murase, O.; Tokuda, H.; Funakoshi, S.; Fujii, N.; Miyajima, K. Biochemistry 1994, 33, 3342–3349.
26. Gutiérrez-Aguirre, I.; Barlic, A.; Zdravko, P.; Macek P.; Anderluh, G.; González-Mañas, J. M. Biochem J 2004, 384, 421–428.
27. Tejuca, M.; Dalla Serra, M.; Ferreras, M.; Lanio, M. E.; Menestrina, G. Biochemistry 1996, 35, 14947–14957.
28. Op den Kamp, J. A. F. Annu Rev Biochem 1979, 48, 47–71.
29. Langner, M.; Kubica, K. Chem Phys Lipids 1999, 101, 3–35.
30. Brockman, H. Curr Opin Struct Biol 1999, 9, 438–443.
31. Martínez, D.; Soto, C.; Casallanovo, F.; Pazos, F.; Alvarez, C.; Lanio, M. E.; Casallanovo, F.; Schreier, S.; Salinas, R. K.; Vergara, C.; Lissi, E. Toxicon 2001, 39, 1547–1560.
32. Wimley, W. C.; Hristova, K. J Membr Biol 2011, 239, 27–34.
33. Chen, R. F.; Knutson, J. R. Anal Biochem 1988, 172, 61–77.
34. Tejuca, M.; Dalla Serra, M.; Potrich, C.; Alvarez, C.; Menestrina, G. J Membr Biol 2001, 183, 125–135.
35. Fasman, G. D. Circular Dichroism and the Conformational Analysis of Biomolecules; Plenum Press: New York, 1996.
36. Lau, S. Y. M.; Taneja, A. K.; Hodges, R. S. J Biol Chem 1984, 259, 13253–13261.
37. Eisenberg, D.; Schwarz, E.; Komaromy, M.; Wall, R. J Mol Biol 1984, 179, 125–142.
38. Monastyrnaya, M.; Leychenko, E.; Isaeva, M.; Likhatskaya, G.; Zelepuga, E.; Kostina, E.; Trifonov, E.; Nurminski, E.; Kozlovskaya, E. Toxicon 2010, 56, 1299–1314.
39. Belmonte, G.; Menestrina, G.; Pederzolli, C.; Krizaj, I.; Gubensek, F.; Turk, T.; Macek, P. Biochim Biophys Acta 1994, 1192, 197–204.
40. Epand, R. Biochim Biophys Acta 2003, 1614, 116–121.
41. Matsuzaki, K.; Sugishita, K.; Ishibe, N.; Ueha, M.; Nakata, S.; Miyajima, K.; Epand, R. Biochemistry 1998, 37, 11856–11863.
42. Haney, E. F.; Nathoo, S.; Vogel, H. J.; Prenner, E. J. Chem Phys Lipids 2010, 163, 82–93.
43. Epand, R. M. Biochim Biophys Acta 1998, 1376, 353–368.
44. Farsad, K.; De Camilli, P. Curr Opin Cell Biol 2003, 15, 372–381.
45. Chen, Y. H.; Yang, J. T.; Chau, K. H. Biochemistry 1974, 13, 3350–3359.